

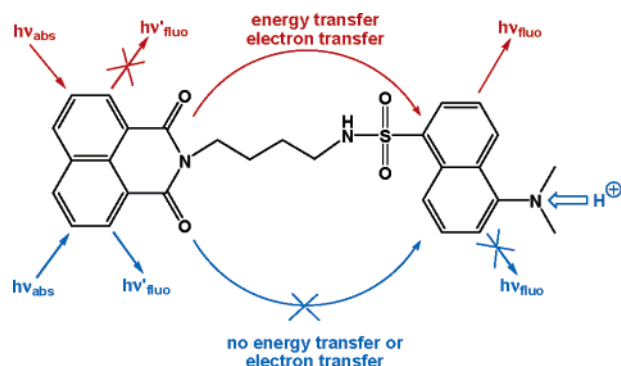
Proton-Induced Fluorescence Switching in Novel Naphthalimide–Dansylamide Dyads

Sergio Abad,[†] Marek Kluciar,[‡] Miguel A. Miranda,[†] and Uwe Pischel^{*‡}

Instituto de Tecnología Química, Universidad Politécnica de Valencia, UPV-CSIC, Av. de los Naranjos s/n, E-46022 Valencia, Spain, and REQUIMTE/Departamento de Química, Universidade do Porto, Rua Campo Alegre, 4169-007 Porto, Portugal

upischel@fc.up.pt

Received June 15, 2005



Three novel bichromophoric dyads containing dansylamide and 1,8-naphthalimide linked by oligomethylene spacers of varying length were prepared. The fluorescent moiety can be reversibly selected by protonation/deprotonation of the dansyl residue via control of singlet–singlet energy transfer and photoinduced electron transfer, leading to a molecular optical switch with two spectrally distinguished “on” states.

The tailored design of photoactive molecular switches showing a defined fluorescence response upon changes in their chemical surrounding, e.g., by addition of protons, has been a topic of considerable interest in recent years.¹ In most cases, the fluorescence of monochromophoric systems has been switched “on” or “off”, by blocking or enabling a transduction mechanism, e.g., photoinduced electron transfer or energy transfer, which allowed communication between the fluorophore and a receptor side.² One step ahead of “on–off” or “off–on” switching is the achievement of control over the photoactivity of a certain fluorophore, i.e., the selection between two different “on” states, in a multichromophoric system. Few examples for such behavior have been realized by using

directional control³ of energy transfer between two photoactive units by protonation, metal cation complexation, temperature change, or electrochemical reduction. This includes an oligophenylenevinylene–phenanthroline dyad⁴ as well as ruthenium(II) polypyridine-containing multicomponent systems linked to anthracene,⁵ catenanes,⁶ or osmium(II) polypyridine complexes and coumarin.⁷

Such systems are foreseen to open new perspectives for the realization of artificial functions at the molecular level. For example, the presence or absence of input information, e.g., of chemical nature, can be translated into the photoactivity of either one of the fluorescent output sites, giving rise to spectrally and spatially distinguished optical signals.⁵ The latter point is an important one, since the induction of site-selective emission distinguishes this conceptual approach from trivial spectral shifts of fluorescence as a result of changes in the chemical surrounding, e.g., solvent polarity, of a fluorophore.⁸

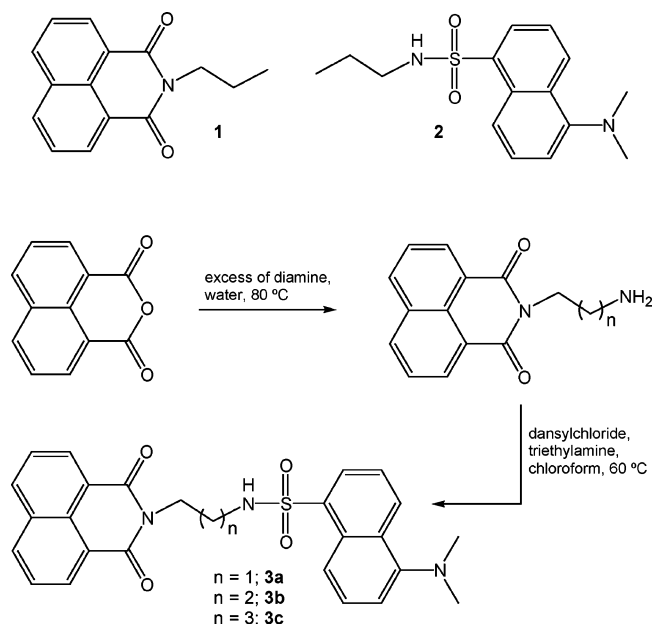
Herein, we report dyads containing two well-known fluorophores, which are widely used in chemosensors and as fluorescent labels: the dansyl (DANS)⁹ and 1,8-naphthalimide (NAPIM) fluorophores.¹⁰ As will be shown below, the selection of these two particular chromophores allows controlling of the fluorescent entity in the dyads

- (2) See, for example: (a) Choi, M.; Kim, M.; Lee, K. D.; Han, K.-N.; Yoon, I.-A.; Chung, H.-J.; Yoon, J. *Org. Lett.* **2001**, *3*, 3455–3457. (b) Gunnlaugsson, T.; Davis, A. P.; O'Brien, J. E.; Glynn, M. *Org. Lett.* **2002**, *4*, 2449–2452. (c) Bu, J.-H.; Zheng, Q.-Y.; Chen, C.-F.; Huang, Z.-T. *Org. Lett.* **2004**, *6*, 3301–3303. (d) Pina, F.; Maestri, M.; Balzani, V.; Vögtle, F. *ChemPhysChem* **2004**, *5*, 473–480. (e) Hanaoka, K.; Kikuchi, K.; Kojima, H.; Urano, Y.; Nagano, T. *J. Am. Chem. Soc.* **2004**, *126*, 12470–12476. (3) Benniston, A. C. *Chem. Soc. Rev.* **2004**, *33*, 573–578. (4) Armaroli, N.; Eckert, J.-F.; Nierengarten, J.-F. *Chem. Commun.* **2000**, 2105–2106. (5) Serroni, S.; Campagna, S.; Pistone Nascone, R.; Hanan, G. S.; Davidson, G. J. E.; Lehn, J.-M. *Chem. Eur. J.* **1999**, *5*, 3523–3527. (6) Cárdenas, D. J.; Collin, J.-P.; Gaviña, P.; Sauvage, J.-P.; De Cian, A.; Fischer, J.; Armaroli, N.; Flamigni, L.; Vicinelli, V.; Balzani, V. *J. Am. Chem. Soc.* **1999**, *121*, 5481–5488. (7) Akasaka, T.; Mutai, T.; Otsuki, J.; Araki, K. *J. Chem. Soc., Dalton Trans.* **2003**, 1537–1544. (8) Suppan, P.; Ghoneim, N. *Solvatochromism*; The Royal Chemical Society: Cambridge, 1997. (9) See, for example: (a) Walkup, G. K.; Imperiali, B. *J. Am. Chem. Soc.* **1997**, *119*, 3443–3450. (b) Prodi, L.; Boletta, F.; Montalti, M.; Zaccheroni, N. *Eur. J. Inorg. Chem.* **1999**, 455–460. (c) Vögtle, F.; Gesterme, S.; Kauffmann, C.; Ceroni, P.; Vicinelli, V.; Balzani, V. *J. Am. Chem. Soc.* **2000**, *122*, 10398–10404. (d) Montalti, M.; Prodi, L.; Zaccheroni, N.; Falini, G. *J. Am. Chem. Soc.* **2002**, *124*, 13540–13546. (e) Vicinelli, V.; Ceroni, P.; Maestri, M.; Balzani, V.; Gorka, M.; Vögtle, F. *J. Am. Chem. Soc.* **2002**, *124*, 6461–6468. (f) Jiang, P.; Chen, L.; Lin, J.; Liu, Q.; Ding, J.; Gao, X.; Guo, Z. *Chem. Commun.* **2002**, 1424–1425. (g) Zheng, Y.; Gattás-Asfura, K. M.; Konka, V.; Leblanc, R. M. *Chem. Commun.* **2002**, 2350–2351. (h) Métivier, R.; Leray, I.; Valeur, B. *Chem. Commun.* **2003**, 996–997. (i) Métivier, R.; Leray, I.; Valeur, B. *Photochem. Photobiol. Sci.* **2004**, *3*, 374–380. (10) See, for example: (a) Daffy, L. M.; de Silva, A. P.; Gunaratne, H. Q. N.; Huber, C.; Lynch, P. L. M.; Werner, T.; Wolfbeis, O. S. *Chem. Eur. J.* **1998**, *4*, 1810–1815. (b) Ramachandram, B.; Saroja, G.; Sankaran, N. B.; Samanta, A. *J. Phys. Chem. B* **2000**, *104*, 11824–11832. (c) Gunnlaugsson, T.; Clive Lee, T.; Parkesh, R. *Org. Biomol. Chem.* **2003**, *1*, 3265–3267. (d) Licchelli, M.; Orbelli Biroli, A.; Poggi, A.; Sacchi, D.; Sangermani, C.; Zema, M. *J. Chem. Soc., Dalton Trans.* **2003**, 4537–4545.

[†] Universidad Politécnica de Valencia.

[‡] Universidade do Porto.

(1) (a) de Silva, A. P.; Gunaratne, H. Q. N.; Gunnlaugsson, T.; Huxley, A. J. M.; McCoy, C. P.; Rademacher, J. T.; Rice, T. E. *Chem. Rev.* **1997**, *97*, 1515–1566. (b) Martínez-Mañez, R.; Sancenón, F. *Chem. Rev.* **2003**, *103*, 4419–4476. (c) Prodi, L. *New J. Chem.* **2005**, *29*, 20–31.

SCHEME 1. Structures of Fluorophore Model Compounds 1 and 2 and Preparation and Structures of Dyads 3a–c


by simple protonation of the dansyl amino nitrogen. Both fluorophores show absorptions in the near-UV and intense fluorescence in the visible region. *N*-Propyl-1,8-naphthalimide (**1**) shows blue fluorescence with $\lambda_{\max} = 376$ nm and characteristic fine structure [$\Phi_f = 0.016$, $\tau_f = 0.145$ ns (for *N*-methyl-1,8-naphthalimide) in MeCN].¹¹ The dansyl chromophore (**2**) is characterized by a strong and broad green fluorescence ($\lambda_{\max} = 507$ nm, $\Phi_f = 0.30$, $\tau_f = 11.2$ ns, in MeCN).¹²

Three dyads (**3a–c**) with two fluorophores connected by oligomethylene spacers of varying length were prepared in a two-step synthesis (cf. Scheme 1): (i) condensation of 1,8-naphthalic anhydride with an excess of diamine yielding a *N*-(aminoalkyl)-1,8-naphthalimide and (ii) linking of the dansyl residue by sulfonamide formation with the free amino group.

Figure 1 shows the fluorescence spectra of the dyads **3a–c** obtained by excitation at 339 nm, where photons are absorbed by both chromophores (29% by DANS and 71% by NAPIM, based on $\epsilon_{339} = 4100$ and $9900 \text{ M}^{-1} \text{ cm}^{-1}$ for DANS and NAPIM, respectively). The typical fluorescence bands of the two chromophores can be observed. However, for dyads with longer spacers (**3b** and **3c**) DANS fluorescence is clearly dominant as compared to dyad **3a** with an ethylene spacer. This is also expressed by the emission efficiency (cf. the Supporting Information for the experimental determination). While its value for NAPIM is $\leq 0.1\%$ for all dyads, for dansyl significant variations are observed: 0.2% for **3a**, 0.9% for **3b**, and 1.5% for **3c**. Remarkably, although NAPIM absorbs the main fraction of photons (71%), its fluorescence is almost negligible, giving rise to visually observable DANS-based

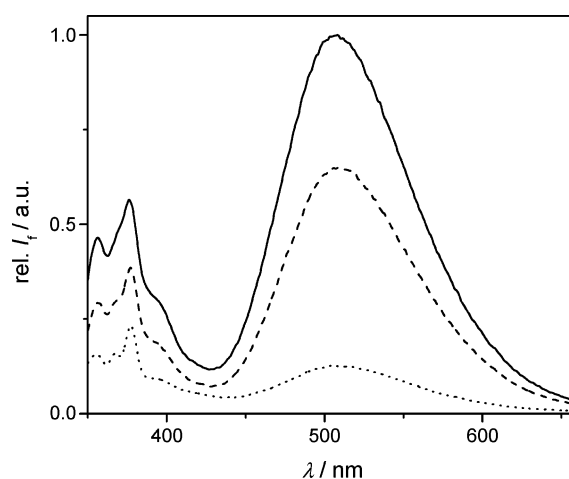
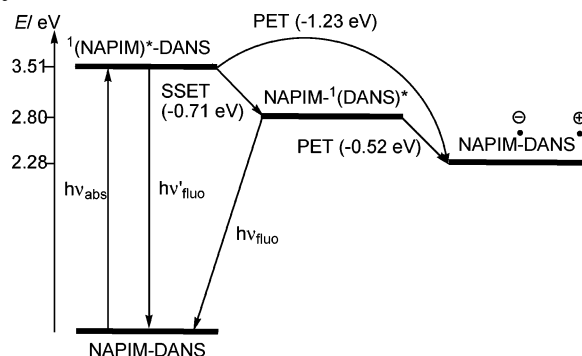


FIGURE 1. Fluorescence spectra ($\lambda_{\text{exc}} = 339$ nm) of optically matched solutions ($A = 0.145$) of dyads **3a** (dotted), **3b** (dashed), and **3c** (full) in acetonitrile.

SCHEME 2. Energy Diagram Describing the Major Photophysical Processes (SSET, PET) in the Dyads 3a


^a The free energy changes are shown in parentheses.¹³

green light emission. However, also the DANS fluorescence is considerably quenched with respect to the model compound **2** ($\Phi_f = 0.30$).

These results can be explained by invoking singlet–singlet energy transfer (SSET) and photoinduced electron transfer (PET) as intramolecular quenching mechanisms. Analysis of the thermodynamic feasibility of these deactivation pathways (cf. Scheme 2) revealed that SSET is only possible in one direction, namely from NAPIM to DANS.

The energy transfer is assumed to proceed via a Coulombic mechanism,¹⁴ which is corroborated by the rather large spectral overlap integral ($J_{\text{Coulombic}} = 3.1 \times 10^{-12} \text{ cm}^6 \text{ mol}^{-1}$). Theoretical calculations (AM1) provide insight into the center-to-center distance between the two chromophores, 5.6, 8.4, and 9.7 Å for **3a**, **b**, and **c**, respectively (cf. Supporting Information), well below the estimated critical energy transfer distance (R_0)¹⁴ of ca.

(13) Free energy changes for PET were calculated with the Rehm–Weller equation: $\Delta G_{\text{PET}} = E_{\text{ox}} - E_{\text{red}} - E_{00} + C$, while $\Delta G_{\text{SSET}} = E_{00}(\text{DANS}) - E_{00}(\text{NAPIM})$ was used to estimate the energetics of the SSET process. The following electrochemical potentials (vs SCE in MeCN) and excited-state energies were used: $E_{\text{ox}}(\text{DANS}) = +0.90$ V, $E_{00}(\text{DANS}) = 2.80$ eV (cf. ref 12); $E_{\text{red}}(\text{NAPIM}) = -1.44$ V, $E_{00}(\text{NAPIM}) = 3.51$ eV (cf. ref 11b). The coulomb term C was taken as -0.06 eV.

(14) Speiser, S. *Chem. Rev.* **1996**, *96*, 1953–1976.

(11) (a) Wintgens, V.; Valat, P.; Kossanyi, J.; Biczok, L.; Demeter, A.; Bérces, T. *J. Chem. Soc., Faraday Trans.* **1994**, *90*, 411–421. (b) Jones, G., II; Kumar, S. *J. Photochem. Photobiol. A* **2003**, *160*, 139–149.

(12) Ceroni, P.; Laghi, I.; Maestri, M.; Balzani, V.; Gestermann, S.; Gorka, M.; Vögtle, F. *New. J. Chem.* **2002**, *26*, 66–75.

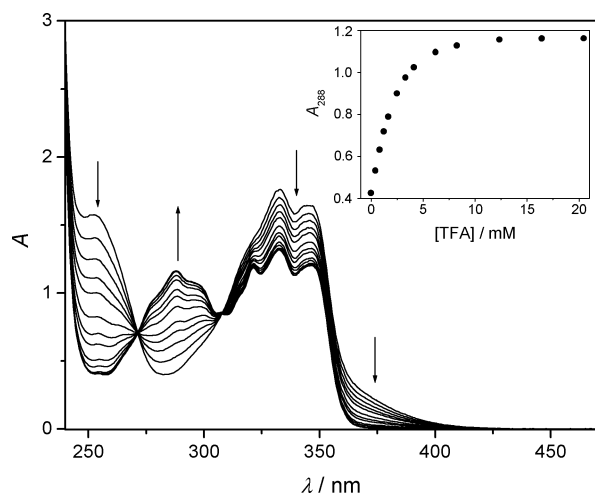


FIGURE 2. Absorption spectra of dyad **3c** (0.1 mM) with different acid concentrations ([TFA] = 0–20.5 mM) in acetonitrile. The inset shows the development at 288 nm.

14.4 Å. This leads to SSET rates in the range of $(0.3\text{--}20) \times 10^{11} \text{ s}^{-1}$, being fastest for the dyad with the shortest spacer (**3a**) and slowest for **3c** with the longest spacer. Further experimental evidence for SSET from NAPIM to DANS was obtained from the excitation spectra ($\lambda_{\text{em}} = 507 \text{ nm}$, where only DANS fluoresces), which clearly displayed the features of the NAPIM chromophore (not shown).

On the other hand, photoinduced electron transfer from the electron-donating DANS to the strong electron acceptor NAPIM is thermodynamically allowed for both excited chromophores (NAPIM via direct excitation, DANS via direct excitation or population via SSET). The rate constant for PET involving singlet-excited DANS can be estimated to k_{et} ca. 10^9 s^{-1} , based on the lifetime of DANS in the model compound **2** ($\tau_f = 11.2 \text{ ns}$) and in dyad **3c** ($\tau_f = 0.6 \text{ ns}$).¹⁵ Further, comparison of the thermodynamics of PET (ΔG_{et} ca. 0.7 eV more favorable for singlet-excited NAPIM; vide supra) indicated that singlet-excited NAPIM should be quenched with rate constants considerably larger than 10^9 s^{-1} .¹⁶

The above-described situation changes completely upon addition of acid to acetonitrile solutions of the dyads. In Figure 2, the dramatic changes in the absorption spectrum of dyad **3c** upon addition of trifluoroacetic acid (TFA) are shown. Akin to the situation observed for the DANS model compound **2**, the long wavelength absorption band related to a n, π^* transition disappears; instead a fine-structured band between 275 and 310 nm can be observed.^{9d,e,i} The latter is ascribed to π, π^* transitions of the naphthalene derivative resulting from protonation of the DANS amino group.

The absorption spectra show two isosbestic points at 271 and 308 nm, clearly indicating the uniform formation of one new species, i.e., the monoprotonated dyad. This is further corroborated by quantitative analysis of the

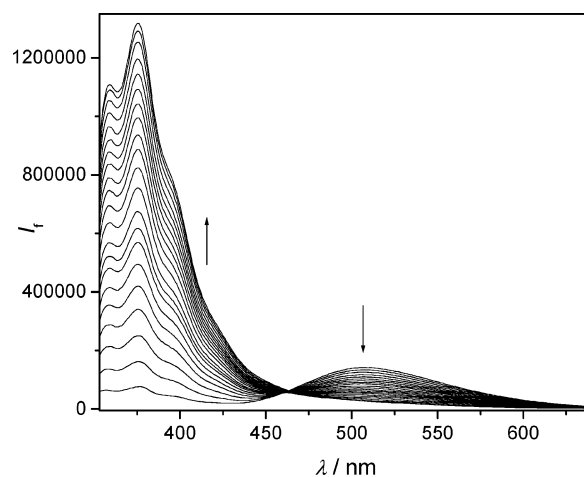


FIGURE 3. Fluorescence titration ($\lambda_{\text{exc}} = 339 \text{ nm}$) of dyad **3c** (0.01 mM) with trifluoroacetic acid (0–5.4 mM) in acetonitrile.

absorption spectra at different acid concentrations with the HYPERQUAD2003 software,¹⁷ which yields a $\log \beta_{11}$ value of 2.7 for all three dyads (**3a–c**) as well as the DANS model compound **2**. This value compares favorably with the one obtained for similar dansyl-containing compounds which yielded $\log \beta_{11} = 2.4$ in acetonitrile/water (60/40) mixtures.⁹ⁱ

Control experiments with model compound **2** showed that protonated DANS does not absorb at 339 nm. Therefore, in the protonated dyads all light is absorbed exclusively by NAPIM. Further, the electron donor capability of DANS is lost and the excited singlet state energy of the formed naphthalene chromophore ($E_S = 3.86 \text{ eV}$; from the intersection of the 0,0 absorption band and the fluorescence of protonated DANS-M, this work; cf. Supporting Information)^{9d,e} is higher than that of NAPIM by 0.35 eV. Thus, electron and energy transfer quenching of singlet-excited NAPIM are not possible, and all excitation energy resides at the imide chromophore, giving rise to its intense and visually observable blue fluorescence. The development of the fluorescence spectrum with increasing acid concentration is shown in Figure 3. The green DANS fluorescence at $\lambda_{\text{max}} = 507 \text{ nm}$ disappears, and at the same time the NAPIM emission at $\lambda_{\text{max}} = 376 \text{ nm}$ is evolving. Noteworthy, tuning of energy transfer efficiency can be also achieved via variations of the donor–acceptor distance as demonstrated for the example of metal complexation by a bichromophoric coumarin dyad with a podand spacer.¹⁸ On the other hand, our system constitutes an example for the total switch-off of energy transfer due to a shift of the acceptor excitation energy and resulting endergonic thermodynamics. This is a clear advantage from the viewpoint of a highly defined output signal, i.e., fluorescence of only one of both output sites.

Additional evidence for the activation of NAPIM excited states upon protonation of the DANS chromophore was obtained by laser flash photolysis studies. Laser

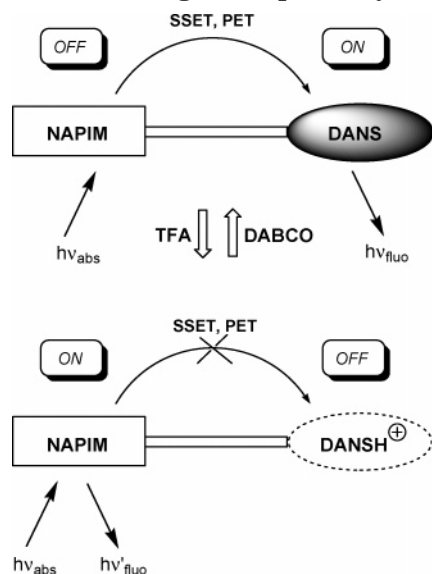
(15) The bimolecular quenching ($\lambda_{\text{exc}} = 375 \text{ nm}$) of the DANS model compound **2** by the NAPIM model compound **1** in acetonitrile proceeds with a diffusion-controlled rate constant ($k_q = 1.7 \times 10^{10} \text{ M}^{-1} \text{ s}^{-1}$).

(16) The experimental determination of accurate rate constants for PET and SSET quenching of singlet-excited NAPIM by DANS in the dyads is complicated by the short fluorescence lifetime of the imide chromophore [0.145 ns for *N*-methyl-1,8-naphthalimide (cf. ref 11a)].

(17) (a) Gans, P.; Sabatini, A.; Vacca, A. *Talanta* **1996**, *43*, 1739–1753. (b) Alderighi, L.; Gans, P.; Ienco, A.; Peters, D.; Sabatini, A.; Vacca, A. *Coord. Chem. Rev.* **1999**, *184*, 311–318.

(18) Valeur, B.; Pouget, J.; Bourson, J.; Kaschke, M.; Ernstring, N. P. *J. Phys. Chem.* **1992**, *96*, 6545–6549. For other examples, see also ref 1a.

SCHEME 3. Switching Principle of Dyads 3



excitation at 308 nm of N_2 -outgassed acetonitrile solutions of the *unprotonated* dyads leads to no signal of triplet–triplet absorption of NAPIM. The highly efficient quenching of singlet-excited NAPIM by energy and electron-transfer excludes notable triplet state population. Instead, the NAPIM radical anion ($\lambda_{\text{max}} = 410$ nm) formed by electron transfer is detected.^{11b} On the other hand, protonation of DANS switches off SSET and PET quenching pathways (see above), leading to NAPIM triplet state population from the singlet-excited state ($\Phi_{\text{ISC}} = 0.94$),^{11a} as evidenced by detection of the characteristic triplet–triplet absorption spectrum with maxima at 360, 440, and 470 nm (cf. the Supporting Information).¹¹

Finally, the system can be switched back in a totally reversible manner by deprotonation of DANSH^+ with a strong organic base [1,4-diazabicyclo[2.2.2]octane (DABCO)]. The initial absorption and fluorescence spectra are recovered upon addition of base (cf. Supporting Information). In other words, energy and electron transfer between NAPIM and DANS can be reversibly controlled as summarized in Scheme 3.

In conclusion, we prepared novel bichromophoric dyads and demonstrated their potential as optical switches for the potential realization of artificial functions at the molecular level. Namely, in comparison to conventional “on–off” or “off–on” systems with one fluorophore, our dyads open a way of converting reversibly chemical input information (acid or base) into two distinct optical output information (fluorescence of NAPIM or DANS) which differ in energy ($\Delta\lambda_{\text{f,max}}$ ca. 130 nm) and space domain.⁵ This is enabled via control of intramolecular energy and electron transfer between two fluorophores. Both interaction mechanisms are switched off for thermodynamic reasons upon protonation of the dansyl unit, which leads to strong blue fluorescence of NAPIM. On the other hand, deprotonated dyads show green fluorescence of DANS. The spectrally well distinguished outputs could be used again as inputs for photoactive molecular devices with different light absorption characteristics leading to optical networks in which the direction of signal transduction can be switched by protonation.¹⁹ Although the emission efficiencies of both chromophores are diminished by competing deactivation processes (ISC, PET), it must be noted that the significant large molar extinction coefficients ϵ balance this disadvantage and lead to overall efficiencies ($\epsilon \times \Phi_f$) which allow both optical output signals to be detected with the naked eye.

Acknowledgment. We thank the Spanish Government, Madrid (Grant No. CTQ 2004-03811 for M.A.M. and doctoral fellowship for S.A.), FCT, Lisbon (Grant No. POCTI/QUI/58535/2004 for U.P. and doctoral fellowship for M.K.), and the Universidad Politécnic de Valencia (Prestige Fellowship for U.P.) for financial support.

Supporting Information Available: Synthetic procedures for **1**, **2**, and **3a–c** and their spectroscopic characterization (^1H and ^{13}C NMR, HRMS, UV/vis data, CHNS analysis), photophysical methodology, laser flash photolysis, UV/vis absorption, and fluorescence spectra of dyads **3a–c** in the presence and absence of TFA, AM1 calculations. This material is available free of charge via the Internet at <http://pubs.acs.org>.

JO0512195

(19) Raymo, F. M.; Giordani, S. *J. Am. Chem. Soc.* **2002**, *124*, 2004–2007.